Tunable crossovers for the quantum interference correction to conductance and shot-noise power in chaotic quantum dots with nonideal contacts

J. G. G. S. Ramos,[1,2] A. L. R. Barbosa,[1,3] and A. M. S. Macêdo[1]

[1]*Departamento de Física, Laboratório de Física Teórica e Computacional, Universidade Federal de Pernambuco 50670-901 Recife, Pernambuco, Brazil*

[2]*Departamento de Física, Universidade Federal da Paraíba, 58051-900 João Pessoa, PB, Brazil*

[3]*Unidade Acadêmica de Educação a Distância e Tecnologia, Universidade Federal Rural de Pernambuco, 52171-900 Recife, Pernambuco, Brazil*

(Received 16 March 2011; published 29 July 2011)

We study a large class of tunable crossovers between the three Dyson universality classes for electron transport through chaotic quantum dots with nonideal contacts. We present analytical expressions for the leading quantum interference corrections to both the conductance and the shot-noise power as a function of the transparencies of the contacts and some tunable crossover parameters, such as a perpendicular magnetic field and spin-orbit coupling strengths. Our results apply both to metallic grains with isotropic spin-orbit coupling and to GaAs heterostructures, in which spin-orbit coupling arises from both the asymmetry of the confining potential and crystal inversion asymmetry. We found that, for nonideal contacts and in the absence of spin-orbit coupling, a perpendicular magnetic field can induce a surprising change of sign in the leading quantum interference correction to the shot-noise power. The results for metallic grains are recovered by independent calculations using quantum circuit theory.

DOI: 10.1103/PhysRevB.84.035453 PACS number(s): 73.23.−b, 73.21.La, 05.45.Mt

I. INTRODUCTION

Electron transport in phase-coherent conductors has many subtle effects resulting from interference patterns of multiply scattered waves. The two most well-known are weak localization (WL) and mesoscopic fluctuations.[1] WL is the leading quantum interference correction to transport observables, such as the conductance, and has proved to be an important source of information on fundamental time scales of the underlying dynamics in finite-size systems. Metal grains are among the simplest realizations of phase-coherent quantum dots, and detailed theoretical descriptions of their transport properties have been obtained from several models and techniques, such as the supersymmetric nonlinear sigma model[2] and random-matrix theory.[3] By applying an external magnetic field and varying its intensity, an ensemble of metal grains interpolates, in the absence of spin-orbit coupling, between two universality classes: the orthogonal class, which describes systems with time-reversal symmetry (TRS), and the unitary class, appropriate for systems with broken TRS. In the presence of spin-orbit coupling, the application of a magnetic field on metal grains induces a crossover from the symplectic class, which describes systems with spin-rotation symmetry (SRS), to the unitary class. More recently, ballistic quantum dots patterned in semiconductor heterostructures have been the subject of intense experimental and theoretical research. The possibility of gate tuning the system's parameters such as spin-orbit coupling and barriers' transparencies has made these devices ideal candidates for systematic studies of quantum interference effects in finite-sized systems in a variety of crossover regimes.

An important transport observable in finite-sized systems is the shot-noise power,[4] which signals the inherent discreteness of the charge carriers in the current. It can also be interpreted quantum mechanically as the second cumulant of the full counting statistics of charge transfer though the system.[5] Recently, the leading quantum interference (or WL) correction to both the shot-noise power[7,8] and the conductance[9,10] have been studied for quantum dots in various crossover regimes. In Refs. 6, 7, and 10, the authors use a trajectory approach to calculate the WL correction to the conductance and shot-noise power in the crossover between the orthogonal and the unitary symmetry classes. In Ref. 9, the framework of random-matrix theory (RMT) is employed to study the general crossover induced by spin-orbit coupling and by an external magnetic field on both the WL correction and the variance of the conductance of a chaotic GaAs quantum dot.[11] An interesting depletion-amplification transition, characterized by a change of sign in the WL correction to the conductance, which can be tuned by the spin-orbit scattering rate, was reported. Changes of sign in the WL correction of a transport observable are always important quantum effects since they signal a qualitative change of behavior in the interference patterns, going from constructive to destructive interference and vice versa. Furthermore, the WL correction is a valuable source of information of the underlying mechanism controlling the coherence of the quantum dynamics in the system and its dependence on fundamental time scales, such as the Ehrenfest time, the phase-coherence time, and the dwell time, emerge naturally from theoretical models of dephasing.[11–13]

In Ref. 8, the authors extended the study of the depletion-amplification transition to the WL correction to the shot-noise power in chaotic quantum dots with ideal contacts. One of the main results of Ref. 8 is the statement that the ratio between the WL correction to the shot-noise power $\langle p^{\mathrm{WL}}\rangle$ and the WL correction to the conductance $\langle g^{\mathrm{WL}}\rangle$ does not depend on crossover parameters and, therefore, does not change sign. This result suggests that the mechanism that fixes the sign of the WL corrections operates equally on both the conductance and the shot-noise power. One of the motivations of this paper

is to extend the above analysis to chaotic quantum dots with barriers.

The presence of barriers or nonideal contacts in chaotic quantum dots can be quite dramatic, as was recently demonstrated in Refs. 14 and 15. It was shown that the electric field manifested in the transparencies of the barriers through gate voltages concomitantly with open scattering channels in the leads can be used to control depletion-amplification transitions in the WL correction to the shot-noise power. In particular, the above-cited ratio $\langle p^{\rm WL}\rangle/\langle g^{\rm WL}\rangle$ can change sign as a function of the barriers' transparencies. In this paper, we address the nontrivial problem of combining the barriers' effect of Refs. 14 and 15 with the crossover effect of Refs. 8 and 9. Our analytical results contain the full recipe for gate tuning the WL corrections to the conductance and the shot-noise power in quantum dots with nonideal contacts.

In Sec. II, we briefly present the random-scattering-matrix formalism of full counting statistics (FCS) and, through a diagrammatic expansion,[9] we perform perturbatively the ensemble average over the scattering-matrix distribution. Our calculations cover both cases: metallic grains with isotropic spin-orbit coupling and ballistic quantum dots patterned in GaAs heterostructures, in which spin-orbit coupling arises from both the asymmetry of the confining potential and crystal inversion asymmetry. Explicit formulas are obtained for the average conductance and the average shot-noise power up to the WL corrections. We observed, in both cases, metallic grains and GaAS quantum dots, a rather surprising effect. For nonideal contacts and in the absence of spin-orbit coupling, a perpendicular magnetic field can induce a change of sign in the leading quantum interference correction to the shot-noise power. In Sec. III, the calculations for metallic grains with nonideal contacts are checked by using quantum circuit theory[16–18] and full agreement is obtained. Finally, in Sec. IV, we present a general discussion of our results highlighting some noteworthy features of the crossover problem in chaotic quantum dots with barriers.

II. SCATTERING-MATRIX FORMALISM

We follow Ref. 19 and introduce a random-scattering-matrix description of the cumulant generating function of the full counting statistics for charge transfer through a double-barrier chaotic quantum dot coupled to two leads, labeled 1 and 2, with N_1 and N_2 open scattering channels, respectively. The FCS generating function is obtained from the scattering-matrix distribution through the following integral transform:

$$\Psi(\vec{\phi}) = \int dS\ \Omega(\vec{\phi},S)P(S), \tag{1}$$

where dS is the Haar measure and $P(S)$ is the scattering-matrix-distribution function. We use the standard parametrization of the scattering matrix and its average

$$S = \begin{pmatrix} r & t' \\ t & r' \end{pmatrix}, \quad \bar{S} = \begin{pmatrix} r_1 & 0 \\ 0 & r_2 \end{pmatrix},$$

where r,r' and t,t' are the dot's reflection and transmission matrices, respectively, and $r_p = \mathrm{diag}(\sqrt{1-T_{p1}},\ldots,\sqrt{1-T_{pN_p}})$ is the reflection matrix of barrier p, which is fully characterized by its transmission coefficients T_{pn}, with $n = 1,\ldots,N_p$. The kernel of the integral transform is given by

$$\Omega(\vec{\phi},S) = \det\left(\frac{1-\sin^2(\phi_0/2)tt^\dagger}{1+\sinh^2(\phi_1/2)tt^\dagger}\right), \tag{2}$$

where $\vec{\phi} \equiv (\phi_0,\phi_1)$. The dimensionless FCS cumulants are obtained from the equation

$$q_{l+1} = \lim_{\varepsilon\to 1}\left(\frac{\varepsilon}{2}\frac{d}{d\varepsilon}\right)^l \left.\frac{\varepsilon^2 I(\phi)}{\sin\phi}\right|_{\cos(\phi/2)=\varepsilon}, \quad l = 0,1,\ldots$$

where $I(\phi)$ is a quantity that plays the role of a pseudocurrent in quantum circuit theory. It is related to $\Psi(\vec{\phi})$ through the equation

$$I(\phi) = -2\left.\frac{\partial\Psi(\vec{\phi})}{\partial\phi_0}\right|_{\vec{\phi}=(\phi,i\phi)}. \tag{3}$$

For later convenience, we give here explicitly the first two FCS cumulants, which are the conductance and the shot-noise power, respectively,

$$\langle g\rangle \equiv q_1 = \langle \mathbf{Tr}[tt^\dagger]\rangle, \tag{4}$$

$$\langle p\rangle \equiv q_2 = \langle \mathbf{Tr}[tt^\dagger(1-tt^\dagger)]\rangle, \tag{5}$$

in which the angle brackets denote the ensemble average over the scattering-matrix distribution.

Averages over random-scattering-matrix ensembles are notably hard to perform. As an example, we mention the exact evaluations of $I(\phi)$, $\langle g\rangle$, $\langle g^2\rangle$, $\langle g^3\rangle$, and $\langle p\rangle$ for the quantum-dot quantum-wire crossover.[20] Here, we use a diagrammatic technique developed in Ref. 21 to perform a perturbative semiclassical expansion of the ensemble average. We begin by introducing a stub parametrization[22] to incorporate the combined effects of barriers, an external magnetic field, and spin-orbit scattering. The stub can be regarded as a mathematical tool to introduce tunable external parameters in the random-scattering-matrix distribution. For particles with spin, the scattering matrix S can be represented as a unitary matrix with quaternionic entries,[23] which can be written as[9]

$$S = TU(1-Q^\dagger RQU)^{-1}T^\dagger, \tag{6}$$

where U is a $M\times M$ unitary symmetric matrix taken from Dyson's circular orthogonal ensemble and the $N\times M$ matrix T carries the relevant information about the barriers. We defined $N = N_1 + N_2$. The $(M-N)\times M$ matrix Q is a projection matrix with $Q_{ij} = \delta_{i+N,j}$. The quaternionic entries of the matrices U, T, and Q are all proportional to the 2×2 unit matrix $\mathbf{1}_2$. The external parameters are introduced in the stub parametrization via a quaternionic $(M-N)\times(M-N)$ unitary matrix R, defined as

$$R(\tau_B,\tau_{\rm SO}) = \exp\left[-i\left(\frac{\mathcal{H}(\tau_B,\tau_{\rm SO})}{M} + iV\mathbf{1}_2\right)\right], \tag{7}$$

where $\mathcal{H}(\tau_B,\tau_{\rm SO})$ is a $(M-N)\times(M-N)$ quaternionic matrix carrying the relevant information about the symmetry breakings and τ_B ($\tau_{\rm SO}$) is the magnetic (spin-orbit) decoherence time. The presence of barriers requires the introduction of an $(M-N)$-dimensional matrix V, which can be constructed from the entries of matrix T. Consistency of the stub method

requires that the limit $M \to \infty$ be taken at the end of the calculations.

A. Effective Hamiltonian model

In this section, we present the effective Hamiltonians $\mathcal{H}(\tau_B,\tau_{\rm SO})$ for metallic grains (isotropic model) and GaAs ballistic quantum dots (anisotropic model). Since these models have already been thoroughly discussed in the recent literature,[9] our presentation will focus only on the most important aspects. The central feature responsible for the simplified random-matrix description of the crossover in the universal regime is the fact that all relevant time scales are much bigger then the electron transit time $\tau_{\rm erg}$, thus $\tau_B,\tau_{\rm SO} \gg \tau_{\rm erg}$. The significance of the crossover effect is guaranteed by the requirement that both τ_B and $\tau_{\rm SO}$ are of the order of the inverse mean level spacing in the cavity or the level broadening due to the presence of barriers. We may thus introduce the following dimensionless parameters to characterize the intensity of symmetry breakings in the system:

$$x^2 = \frac{2\pi\hbar}{\tau_B \Delta}, \quad a^2 = \frac{2\pi\hbar}{\tau_{\rm SO}\Delta}, \tag{8}$$

where Δ is the mean level spacing.

The random-matrix models for the effective Hamiltonians then follow directly from general symmetry considerations. They are given by

$$\mathcal{H}_{\rm iso}(\tau_B,\tau_{\rm SO}) = ix\ X\ \mathbf{1}_2 + \frac{i\ a}{\sqrt{2}}\ \sum_{i=1}^{3} A_i\ \sigma_i \tag{9}$$

for metallic grains, and

$$\mathcal{H}_{\rm aniso}(\tau_B,\tau_{\rm SO}) = ix\ X\ \mathbf{1}_2 + i\ a\ \sum_{i=1}^{2} A_i\ \sigma_i \tag{10}$$

for ballistic quantum dots patterned in GaAs heterostructures. In the above equations, X and A_i $(i = 1,2,3)$ are real antisymmetric matrices of dimension $(M-N)\times(M-N)$ and σ_i are Pauli matrices. The entries of these matrices are independent Gaussian random numbers with vanishing average $\langle \mathbf{Tr}(X)\rangle = \langle \mathbf{Tr}(A_i)\rangle = 0$, and with variances given by $\langle \mathbf{Tr}(XX^T)\rangle = M^2$ and $\langle \mathbf{Tr}(A_i A_j^T)\rangle = \delta_{ij} M^2$.

B. Average conductance

We are now in position to perform the diagrammatic perturbative expansion of the average conductance $\langle g\rangle$ in inverse powers of N and M. The first term contributing to $\langle g\rangle$ is obtained by adding ladder-type diagrams. For this term, we may neglect the contribution from the matrix $\mathcal{H}(\tau_B,\tau_{\rm SO})$ and Eq. (7) simplifies to

$$R = e^{V\mathbf{1}_2}, \tag{11}$$

with $Q^\dagger R Q \otimes Q^\dagger R^\dagger Q = \mathbf{1}\otimes\mathbf{1} - T^\dagger \otimes T$, where the matrix $T^\dagger T$ has eigenvalues, denoted Γ_n, which represent the transparencies of the barriers. We shall neglect, for simplicity, any channel dependence on the barriers' transparencies. To perform the trace over the channel indices, we use the following identity: $\mathbf{Tr}(R\otimes R^\dagger) = (M - N_1\Gamma_1 - N_2\Gamma_2)\mathbf{1}_2 \otimes \mathbf{1}_2$. By selecting and adding the ladder-type diagrams, we obtain

$$\langle g\rangle = \sum_{\rho\sigma} \{[\mathbf{Tr}\,(C_1)\,\mathbf{Tr}\,(C_2)]\,\mathcal{D}\}_{\rho\sigma;\sigma\rho} = 2\frac{G_1 G_2}{G_1+G_2}, \tag{12}$$

where $G_i = N_i\Gamma_i$, $C_i = W_i T \otimes W_i^\dagger T^\dagger$, $\mathbf{Tr}(C_i) = G_i \mathbf{1}_2\otimes\mathbf{1}_2$, and

$$\mathcal{D} = [M\mathbf{1}_2\otimes\mathbf{1}_2 - \mathbf{Tr}(R\otimes R^\dagger)]^{-1}, \tag{13}$$

in agreement with Ref. 21. The tensor multiplications must be understood by means of the rule[9]

$$(\sigma_i\otimes\sigma_j)(\sigma_k\otimes\sigma_l) = (\sigma_i\sigma_k\otimes\sigma_l\sigma_j), \tag{14}$$

and the factor 2 is due to spin degeneracy.

The next term in the expansion is called the weak-localization correction. It is composed of two contributions. The first one, denoted δg_1, is obtained from the ladder diagrams by applying the following correction to the weight[21] $M^{-n} \longrightarrow M^{-n} - nM^{-n-1}$. We get

$$\delta g_1 = -\sum_{\rho\sigma}\{[\mathbf{Tr}(C_1)\mathbf{Tr}(C_2)]\mathcal{D}^2\}_{\rho\sigma;\sigma\rho} = -2\frac{G_1G_2}{(G_1+G_2)^2}. \tag{15}$$

The second contribution to the weak-localization term comes from the summation of a class of diagrams that have both ladder and crossed parts.[21] We remark that only the crossed portions of these Cooperon-type diagrams are affected by a magnetic field and/or spin-orbit scattering. The expression obtained from this contribution reads as

$$\begin{aligned}\delta g_2 = \sum_{\rho\sigma}\{&-(M^{-3}\mathbf{1}_2\otimes\mathbf{1}_2)\mathbf{Tr}[F_L(\mathcal{T}f_{TT}\mathcal{T})]\mathbf{Tr}[F_R]\\ &+\mathbf{Tr}[F_L(\mathcal{T}f_{UU}\mathcal{T})F_R]\}_{\rho\sigma;\rho\sigma},\end{aligned} \tag{16}$$

where $\mathcal{T} = \mathbf{1}_2\otimes\sigma_2$,

$$\begin{aligned}F_L &= C_1 + \mathbf{Tr}\,[C_1]\,\mathcal{D}(R^\dagger\otimes R),\\ F_R &= C_2 + (R\otimes R^\dagger)\mathbf{Tr}\,[C_2]\,\mathcal{D},\end{aligned}$$

and

$$\begin{aligned}f_{UU} &= [M\mathbf{1}_2\otimes\mathbf{1}_2 - \mathbf{Tr}(R\otimes R^*)]^{-1},\\ f_{TT} &= (M\mathbf{1}_2\otimes\mathbf{1}_2)\mathbf{Tr}(R\otimes R^*)f_{UU}.\end{aligned}$$

The superscript $*$ denotes the quaternion complex conjugation. By using Eqs. (7), the conjugation rules of quaternions and taking the limit $M\longrightarrow\infty$, we obtain

$$f_{UU}^{-1} = \left(G_C + \frac{3}{2}\,a^2\right)\mathbf{1}_2\otimes\mathbf{1}_2 - \frac{a^2}{2}\ \sum_{i=1}^{3}\sigma_i\otimes\sigma_i \tag{17}$$

for the isotropic model and

$$f_{UU}^{-1} = (G_C + 2\,a^2)\mathbf{1}_2\otimes\mathbf{1}_2 - a^2\ \sum_{i=1}^{2}\sigma_i\otimes\sigma_i \tag{18}$$

for the anisotropic model with $G_C = G_1 + G_2 + 2x^2$. By summing Eqs. (12), (15), and (16), we find the following expression for the average conductance for the isotropic and

anisotropic models, respectively:

$$\langle g_{\rm iso}\rangle = 2\frac{G_1G_2}{G_1+G_2}\left[1-\frac{(G_1\Gamma_2+G_2\Gamma_1)}{(G_1+G_2)}\left(\frac{1}{G_C+2a^2}-\frac{a^2}{G_C(G_C+2a^2)}\right)\right], \tag{19}$$

$$\langle g_{\rm aniso}\rangle = 2\frac{G_1G_2}{G_1+G_2}\left[1-\frac{(G_1\Gamma_2+G_2\Gamma_1)}{2(G_1+G_2)}\left(\frac{1}{G_C+2a^2}+\frac{1}{G_C+4a^2}-\frac{2a^2}{G_C(G_C+2a^2)}\right)\right]. \tag{20}$$

These equations are the central results of this section. They contain the combined contributions of magnetic field, spin-orbit scattering, and barriers of arbitrary transparencies to the average conductance of a quantum dot with nonideal contacts. The leading terms in both equations are classical contributions, while the subleading terms are dominant quantum interference corrections. As an important check, we set $\Gamma_1=\Gamma_2=1$ in Eq. (20) and it yields the result obtained in Ref. 9. In Fig. 1, we plot the weak-localization terms of both Eqs. (19) and (20) as a function of the magnetic field parameter x for several fixed values of the spin-orbit parameter a. Comparing the isotropic model (full lines) with the anisotropic one (symbols), we see an overall qualitative agreement and only a small quantitative difference between the results at intermediate values of the spin-orbit parameter a. Finally, Eq. (19) shows that the presence of the tunnel barriers generates, in both the isotropic and anisotropic models, a linear suppression to the weak-localization correction in the opaque limit, defined in Ref. 24 through the limit $\Gamma_i\to 0$ with G_i fixed, for all values of the magnetic field and the spin-orbit scattering parameters. This behavior, according to the semiclassical trajectory-based approach of Ref. 24, occurs due to a competition between tunneling and interference, two fundamental aspects of quantum mechanics. It is interesting to point out that, in the semiclassical trajectory-based approach, quantum corrections to any observable arise from loops that are added in the corresponding "classical" leading diagram.[25,26]

C. Average shot-noise power

We now turn to the diagrammatic perturbative expansion of the average shot-noise power $\langle p\rangle$. The essential idea is to employ the decomposition $\langle p\rangle=\langle g\rangle-\langle h\rangle$, where $h\equiv\mathbf{Tr}(tt^\dagger)^2$ and then apply to $\langle h\rangle$ the same scheme described in Sec. II B. Interestingly, one can use in the crossover problem of a quantum dot with nonideal contacts the same diagrams that appear in the pure orthogonal class. A detailed account of the whole set of diagrams can be found in Ref. 15. The calculation is straightforward, albeit somewhat cumbersome. Here, we show only the final result, which reads as

$$\begin{aligned}\langle p_{\rm iso}\rangle = {}& 2G_1G_2\left[G_1G_2(G_1+G_2)+G_1^3(1-\Gamma_2)+G_2^3(1-\Gamma_1)\right]/[G_1+G_2]^4+2G_1G_2(G_1\Gamma_2+G_2\Gamma_1)[A_{6,0}x^6+A_{4,2}x^4a^2\\ &+A_{2,4}x^2a^4+A_{4,0}x^4+A_{0,4}a^4+A_{2,2}x^2a^2+A_{2,0}x^2+A_{0,2}a^2+A_{0,0}]/\left[G_C^2(G_1+G_2)^5(G_C+2a^2)^2\right]\end{aligned} \tag{21}$$

for the isotropic model, with $A_{i,j}$ shown in Eq. (A1), and

$$\begin{aligned}\langle p_{\rm aniso}\rangle = {}& 2G_1G_2\left[G_1G_2(G_1+G_2)+G_1^3(1-\Gamma_2)+G_2^3(1-\Gamma_1)\right]/[G_1+G_2]^4+2G_1G_2(\Gamma_2G_1+\Gamma_1G_2)[B_{10,0}x^{10}\\ &+B_{8,2}x^8a^2+B_{2,8}x^2a^8+B_{8,0}x^8+B_{0,8}a^8+B_{6,4}x^6a^4+B_{4,6}x^4a^6+B_{6,2}x^6a^2+B_{2,6}x^2a^6+B_{6,0}x^6+B_{0,6}a^6\\ &+B_{4,4}x^4a^4+B_{4,2}x^4a^2+B_{2,4}x^2a^4+B_{4,0}x^4+B_{0,4}a^4+B_{2,2}x^2a^2+B_{2,0}x^2+B_{0,2}a^2+B_{0,0}]/\\ &[(G_C+4a^2)^2(G_C+2a^2)^2(G_C)^2(G_1+G_2)^5]\end{aligned} \tag{22}$$

for the anisotropic model, with $B_{i,j}$ shown in Eq. (A2). These equations are the central results of this section. They contain the combined contributions of magnetic field, spin-orbit scattering, and barriers of arbitrary transparencies to the average shot-noise power of a quantum dot with nonideal contacts. If we set $\Gamma_1=\Gamma_2=1$ in Eq. (22), we recover the result obtained in Ref. 27. As a further test, we set $x=a=0$ and recover the result obtained in Refs. 14 and 15. Note that, in the opaque limit defined in Sec. II B, the WL correction to shot-noise power tends linearly to zero, as expected. In Fig. 2, we show the general behavior of the WL correction in both the isotropic (full lines) and the anisotropic (symbols) models as a function of the magnetic field parameter x for several fixed values of the spin-orbit parameter a. We see again an overall qualitative agreement between the models with only a small quantitative difference showing up at intermediate values of the spin-orbit parameter a.

The results of Eq. (21) can be best understood through diagrams in the planes (x,a) and (Γ_1,Γ_2) for fixed $N_2/N_1\approx 0.67$, as shown in Fig. 3. The most important feature is the existence of regions in parameter space denoted $(-)$ and $(+)$ in Figs. 3(c) and 3(d), where $\langle p^{\rm WL}\rangle<0$ and $\langle p^{\rm WL}\rangle>0$, respectively. Consequently, a system subject to a weak perpendicular magnetic field exhibits depletion-amplification transitions in the quantum correction to the average shot-noise power. Note that the region that was positive $(+)$ in Fig. 3(c) becomes negative $(-)$ in Fig. 3(d) and vice versa. Figure 3(e) shows the orthogonal-symplectic crossover for $x=0$.

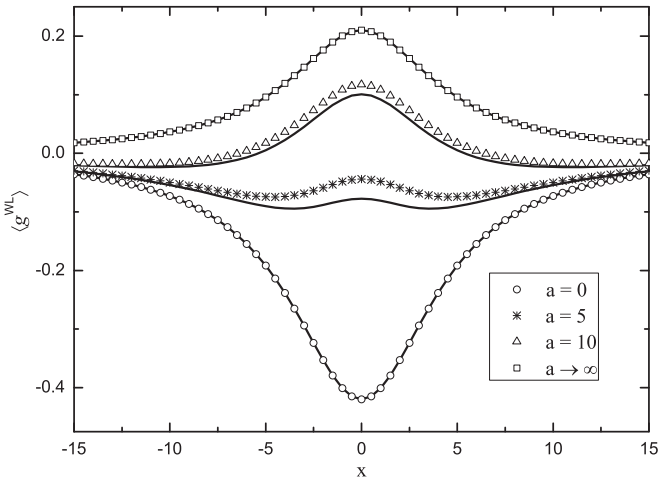

FIG. 1. Weak-localization correction to the average conductance as a function of the magnetic field parameter x for fixed values of the spin-orbit parameter a. The full lines correspond to the isotropic model, while the symbols correspond to the anisotropic model. In both cases, we used $\Gamma_1 = 0.8$, $\Gamma_2 = 0.9$, and $N_2/N_1 \approx 0.67$.

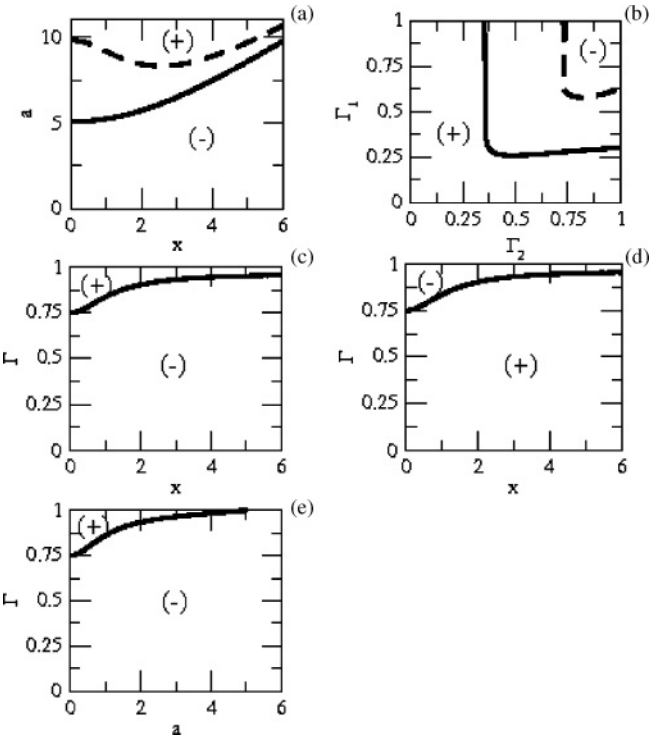

FIG. 3. Diagrams showing the depletion-amplification transition for $N_2/N_1 \approx 0.67$. (a) Diagrams (x, a) separating positive (+) (amplification) and negative (−) (depletion) regions for $\Gamma_1 = 1$ with $\Gamma_2 = 0{,}3$ (continuous lines) and $\Gamma_2 = 0{,}7$ (dashed lines); (b) positive (+) and negative (−) regions in the plane (Γ_1, Γ_2) for $x = 2$ with $a = 6$ (continuous lines) and $a = 10$ (dashed lines); (c) diagram in the plane (Γ, x), obtained by setting $\Gamma_1 = \Gamma_2 = \Gamma$ and by taking the limit $a \to 0$; (d) diagram similar to (c), obtained by taking the limit $a \to \infty$; (e) diagram in the plane (Γ, a), obtained by setting $\Gamma_1 = \Gamma_2 = \Gamma$ and by taking the limit $x \to 0$.

III. CIRCUIT THEORY

Considering the complexity of the analytical expressions for the average shot-noise power shown in the preceding section, we found it wise to check it via an independent method. A technique that stands out for its simplicity is quantum circuit theory (QCT).[16–18] In its present form, QCT can deal only with the isotropic model. Our calculations are based on a recent extension of QCT (Ref. 28) to account for weak-localization corrections to quantum transport observables. The starting point of QCT is the basic conservation law of pseudocurrents $I(\phi) = I_1(\phi - \chi) = I_2(\chi)$, where I_1 and I_2 represent the pseudocurrents at leads 1 and 2, respectively, ϕ is a fictitious pseudopotential at one of the reservoirs, and χ is the value of the pseudopotential at the quantum dot. The effect of the barriers is introduced via the following "current-voltage" relations:

$$I_p(\phi) = \sum_{n=1}^{N_p} \frac{2\Gamma_{pn}\tan(\phi/2)}{1 + (1 - \Gamma_{pn})\tan^2(\phi/2)}, \quad p = 1,2. \quad (23)$$

The basic idea for the calculation of WL corrections within QCT is the interpretation of the pseudocurrent conservation law as a saddle-point approximation to a certain functional integral. Fluctuations around this dominant saddle-point term are interpreted as quantum interference corrections. We may thus introduce an expansion in inverse powers of the classical conductance as follows: $I^{(\beta)}(\phi) = I_{\rm sp}(\phi) + I^{\rm WL}(\phi) + \cdots$ with $I_{\rm sp}$ and $I^{\rm WL}$ denoting the saddle-point solution and the WL correction, respectively. For quantum dots with arbitrary contacts and in the presence of both magnetic field and spin-orbit scattering, Campagnano and Nazarov[28] were able to obtain an equation for $I^{\rm WL}(\phi)$, which in our notation reads as

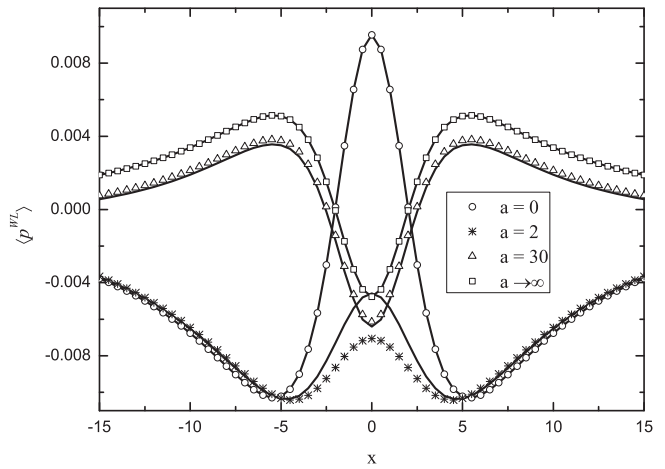

FIG. 2. Weak-localization correction to the average shot-noise power as a function of the magnetic field parameter x for fixed values of the spin-orbit parameter a. The full lines correspond to the isotropic model, while the symbols correspond to the anisotropic model. In both cases, we used $\Gamma_1 = 0.8$, $\Gamma_2 = 0.9$, and $N_2/N_1 \approx 0.67$. Note the change of sign in the WL correction as a function of x.

$$I^{\mathrm{WL}}(\phi) = \frac{1}{2}\frac{d}{d\phi}\left[\ln\left(\frac{M_+(\phi)+4x^2}{M_-(\phi)+4x^2}\right) + 3\ln\left(\frac{M_+(\phi)+4x^2+4a^2}{M_-(\phi)+4x^2+4a^2}\right)\right], \quad (24)$$

where x and a are defined as in Sec. II A. The auxiliary functions $M_\pm(\phi)$ are given by

$$M_+(\phi) = 2\frac{I'_{sp}(\phi)}{1/4-[\chi'(\phi)]^2}$$

$$M_-(\phi) = 2I_{sp}(\phi)\left[\cot\left(\chi(\phi)+\frac{\phi}{2}\right)-\cot\left(\chi(\phi)-\frac{\phi}{2}\right)\right],$$

with $I'_{sp}(\phi) \equiv dI_{sp}(\phi)/d\phi$. The intermediate phase function $\chi(\phi)$ is obtained by solving the saddle-point equation $I_{sp}(\phi) = I_1(\phi/2+\chi) = I_2(\phi/2-\chi)$. For equivalent channels $\Gamma_{pn} = \Gamma_p$, the above conservation law yields a polynomial equation of fourth degree. A subtle technical detail of this procedure is the selection of the physical root of this equation, which, after being inserted into Eq. (24), yields the explicit form of the current-voltage relation $I(\phi)$. The average conductance and the average shot-noise power are then obtained from the relations

$$\langle g_{\mathrm{iso}}\rangle = \frac{\cos^2(\phi/2)}{\sin(\phi)}I(\phi)\Big|_{\phi=0},$$

$$\langle p_{\mathrm{iso}}\rangle = -\cot(\phi/2)\frac{d}{d\phi}\left(\frac{\cos^2(\phi/2)}{\sin(\phi)}I(\phi)\right)\Big|_{\phi=0}. \quad (25)$$

We carried out this calculation and obtained results that are in full agreement with those presented in previous sections.

IV. DISCUSSION AND CONCLUSIONS

In Figs. 1 and 2, we showed the WL correction to the average conductance and the average shot-noise power [Eqs. (19) and (21), respectively] as a function of magnetic field parameter x and spin-orbit parameter a. Note that, in $\langle g^{\mathrm{WL}}\rangle$, the depletion-amplification effect, i.e., a change of sign, occurs by varying a with fixed x, which corresponds to the standard crossover between universality classes. On the other hand, we observe an unexpected depletion-amplification effect in $\langle p^{\mathrm{WL}}\rangle$ as a function of x when $a = 0$ (orthogonal-unitary crossover) and $a \to \infty$ (symplectic-unitary crossover). This means that, in order to amplify or deplete the dominant semiclassical contribution to the shot-noise power, we do not need in general to change the rate of spin-orbit scattering. The intensity of the general crossover depends jointly on the number of open scattering channels in the leads, on the barriers' transparencies, on the magnetic field parameter x, and on the spin-orbit parameter a.

A detailed analysis of the crossover in the particular case of ideal contacts was presented by Béri and Cserti[8] and, more recently, by Saito and Nagao.[29] They found the very simple relation

$$\frac{\langle p^{\mathrm{WL}}\rangle}{\langle g^{\mathrm{WL}}\rangle} = -\left(\frac{N_1-N_2}{N_1+N_2}\right)^2, \quad (26)$$

which we reproduce by setting $\Gamma_1 = \Gamma_2 = 1$ in Eqs. (19) and (21). The remarkable aspect of Eq. (26) is that it is universal in the sense that it is independent of the crossover parameters x and a. We observe, however, that in the presence of tunnel barriers, the ratio $\langle p^{\mathrm{WL}}\rangle/\langle g^{\mathrm{WL}}\rangle$ always depends on the crossover parameters and the universality is broken. Another noteworthy feature about $\langle p^{\mathrm{WL}}\rangle/\langle g^{\mathrm{WL}}\rangle$ is that it is not suppressed in the opaque limit. For instance, if we take the opaque limit and set $x = 0 = a$, we obtain

$$\frac{\langle p^{\mathrm{WL}}\rangle}{\langle g^{\mathrm{WL}}\rangle} = -\frac{3G_1G_2(G_1-G_2)\left(G_2^2-G_1^2\right)}{(G_1+G_2)^2}. \quad (27)$$

From a conceptual point of view, the results presented in this paper provide a powerful test for comparing different theoretical approaches to quantum transport, such as quantum circuit theory, the supersymmetric nonlinear σ model, the random-scattering-matrix approach, and the trajectory-based semiclassical theory. Furthermore, our results exhibit an interesting and nontrivial competition between tunneling and interference, which can be controlled experimentally by varying an external magnetic field and gate-voltage-induced spin-orbit scattering. We also would like to remark that many of the transitions predicted in this paper could become useful tools to detect, in a controlled way, the weak-localization correction to conductance and shot-noise power in ballistic chaotic quantum dots. Experiments with tunable barriers, such as those presented in Refs. 30–32, are already able to detect small variations in the electric current and in this way extract both the full counting statistics and cumulants up to the fifth order. Gate-controlled spin-orbit scattering has also been used as tools to monitor quantum interference effects, such as in Refs. 33 and 34. As a final remark, we point out that, although the effect predicted in this paper is harder to detect than the shot-noise power itself, since in general $\langle p^{\mathrm{WL}}\rangle/\langle p\rangle \sim 1/N$, and numerical simulations indicate the onset of the semiclassical regime around $N \sim 50$, one can see from Eqs. (26) and (27) that the effect can be considerably enhanced by tuning the contact conductances $G_i = N_i\Gamma_i$ of the barriers.

ACKNOWLEDGMENTS

This work was partially supported by CNPq, CAPES, and FACEPE (Brazilian Agencies). We thank P. W. Brouwer for discussions and suggestions.

APPENDIX

We give below explicit expressions for the A and B coefficients shown in Eqs. (21) and (22)

$$A_{6,0} = 8\left[-G_1G_2(G_1+G_2) - 3\left(G_1^3+G_2^3\right) + 4\left(G_2^3\Gamma_1+G_1^3\Gamma_2\right)\right],$$

$$A_{4,2} = 4\left[-G_1G_2(G_1+G_2) - 3\left(G_1^3+G_2^3\right) + 4\left(G_2^3\Gamma_1+G_1^3\Gamma_2\right)\right],$$

$$A_{2,4} = -4\left[-G_1G_2(G_1+G_2) - 3\left(G_1^3+G_2^3\right) + 4\left(G_2^3\Gamma_1+G_1^3\Gamma_2\right)\right],$$

$$A_{4,0} = 4(G_1+G_2)\left[12\left(G_1^3\Gamma_2+G_2^3\Gamma_1\right) - 9\left(G_1^3+G_2^3\right) + G_1G_2(G_1+G_2) - 4G_1G_2(G_1\Gamma_2+G_2\Gamma_1)\right],$$

$$
\begin{aligned}
A_{0,4} &= -2(G_1-G_2)(G_1+G_2)\left[4\left(G_1^2\Gamma_2-\Gamma_1G_2^2\right)+3\left(G_2^2-G_1^2\right)\right],\\
A_{2,2} &= 4(G_1+G_2)^2\left[4\left(G_1^2\Gamma_2+G_2^2\Gamma_1\right)-3\left(G_1^2+G_2^2\right)-2G_1G_2\right],\\
A_{2,0} &= 2(G_1+G_2)^2\left[12\left(G_1^3\Gamma_2+G_2^3\Gamma_1\right)-9\left(G_1^3+G_2^3\right)+5G_1G_2(G_1+G_2)-8G_1G_2(G_1\Gamma_2+G_2\Gamma_1)\right],\\
A_{0,2} &= (G_1+G_2)^2\left[-3\left(G_1^3+G_2^3\right)+4\left(G_2^3\Gamma_1+G_1^3\Gamma_2\right)-9G_1G_2(G_1+G_2)+8G_1G_2(G_1\Gamma_2+G_2\Gamma_1)\right],\\
A_{0,0} &= (G_1-G_2)(G_1+G_2)\left[4\left(G_1^2\Gamma_2-\Gamma_1G_2^2\right)+3\left(G_2^2-G_1^2\right)\right],
\end{aligned}
\tag{A1}
$$

$$
\begin{aligned}
B_{0,0} &= (G_1-G_2)(G_1+G_2)^5\left[4\left(G_1^2\Gamma_2-\Gamma_1G_2^2\right)-3\left(G_1^2-G_2^2\right)\right],\\
B_{2,8} &= 192G_2^3-256\Gamma_2G_1^3-256\Gamma_1G_2^3+64G_2^2G_1+64G_2G_1^2+192G_1^3,\\
B_{0,8} &= -32(G_1-G_2)(G_1+G_2)\left[4\left(G_1^2\Gamma_2-\Gamma_1G_2^2\right)-3\left(G_1^2-G_2^2\right)\right],\\
B_{4,6} &= 96G_2^3+96G_1^3-128\Gamma_2G_1^3+32G_2G_1^2-128\Gamma_1G_2^3+32G_2^2G_1,\\
B_{2,6} &= -32(G_1+G_2)\left(4\Gamma_2G_1^3-3G_1^3+11G_2G_1^2-12G_1^2\Gamma_2G_2-12G_1\Gamma_1G_2^2+11G_2^2G_1-3G_2^3+4\Gamma_1G_2^3\right),\\
B_{0,6} &= -8(G_1+G_2)^2\left(4\Gamma_2G_1^3-3G_1^3+23G_2G_1^2-24G_1^2\Gamma_2G_2+23G_2^2G_1-24G_1\Gamma_1G_2^2-3G_2^3+4\Gamma_1G_2^3\right),\\
B_{6,4} &= -384G_2^3-384G_1^3+512\Gamma_1G_2^3-128G_2^2G_1-128G_2G_1^2+512\Gamma_2G_1^3,\\
B_{4,4} &= 64(G_1+G_2)\left(-9G_1^3+12\Gamma_2G_1^3+2G_1^2\Gamma_2G_2-5G_2G_1^2+2G_1\Gamma_1G_2^2-5G_2^2G_1-9G_2^3+12\Gamma_1G_2^3\right),\\
B_{2,4} &= 32(G_1+G_2)^2\left(-9G_1^3+12\Gamma_2G_1^3-7G_2G_1^2+4G_1^2\Gamma_2G_2+4G_1\Gamma_1G_2^2-7G_2^2G_1-9G_2^3+12\Gamma_1G_2^3\right),\\
B_{0,4} &= 16(G_1+G_2)^3\left(-3G_1^3+4\Gamma_2G_1^3-3G_2G_1^2+2G_1^2\Gamma_2G_2-3G_2^2G_1+2G_1\Gamma_1G_2^2-3G_2^3+4\Gamma_1G_2^3\right),\\
B_{8,2} &= -384G_2^3-384G_1^3+512\Gamma_1G_2^3-128G_2^2G_1-128G_2G_1^2+512\Gamma_2G_1^3,\\
B_{6,2} &= 128(G_1+G_2)\left(-6G_1^3+8\Gamma_2G_1^3-G_1^2\Gamma_2G_2-G_2G_1^2-G_1\Gamma_1G_2^2-G_2^2G_1+8\Gamma_1G_2^3-6G_2^3\right),\\
B_{4,2} &= 192(G_1+G_2)^2\left(-3G_1^3+4\Gamma_2G_1^3-G_1^2\Gamma_2G_2-G_1\Gamma_1G_2^2-3G_2^3+4\Gamma_1G_2^3\right),\\
B_{2,2} &= 32(G_1+G_2)^3\left(-6G_1^3+8\Gamma_2G_1^3-3G_1^2\Gamma_2G_2+G_2G_1^2+G_2^2G_1-3G_1\Gamma_1G_2^2+8\Gamma_1G_2^3-6G_2^3\right),\\
B_{0,2} &= 8(G_1+G_2)^4\left(-3G_1^3+4\Gamma_2G_1^3+G_2G_1^2-2G_1^2\Gamma_2G_2-2G_1\Gamma_1G_2^2+G_2^2G_1-3G_2^3+4\Gamma_1G_2^3\right),\\
B_{10,0} &= -32G_2G_1^2+128\Gamma_2G_1^3-96G_1^3-96G_2^3+128\Gamma_1G_2^3-32G_2^2G_1,\\
B_{8,0} &= 16(G_1+G_2)\left(-15G_1^3+20\Gamma_2G_1^3-4G_1^2\Gamma_2G_2-G_2G_1^2-4G_1\Gamma_1G_2^2-G_2^2G_1+20\Gamma_1G_2^3-15G_2^3\right),\\
B_{6,0} &= 16(G_1+G_2)^2\left(-15G_1^3+20\Gamma_2G_1^3-8G_1^2\Gamma_2G_2+3G_2G_1^2+3G_2^2G_1-8G_1\Gamma_1G_2^2+20\Gamma_1G_2^3-15G_2^3\right),\\
B_{4,0} &= 8(G_1+G_2)^3\left(-15G_1^3+20\Gamma_2G_1^3+7G_2G_1^2-12G_1^2\Gamma_2G_2-12G_1\Gamma_1G_2^2+7G_2^2G_1+20\Gamma_1G_2^3-15G_2^3\right),\\
B_{2,0} &= 2(G_1+G_2)^4\left(-15G_1^3+20\Gamma_2G_1^3+11G_2G_1^2-16G_1^2\Gamma_2G_2-16G_1\Gamma_1G_2^2+11G_2^2G_1+20\Gamma_1G_2^3-15G_2^3\right).
\end{aligned}
\tag{A2}
$$

[1] For a review, see E. Akkermans and G. Montambaux, *Mesoscopic Physics of Electrons and Photons* (Cambridge University Press, Cambridge, 2006).

[2] K. Efetov, *Supersymmetry in Disorder and Chaos* (Cambridge University Press, Cambridge, 2006).

[3] For a review, see T. Guhr, A. Müller-Groeling, and H. A. Weidenmüller, Phys. Rep. **299**, 189 (1998).

[4] Ya. M. Blanter and M. Buttiker, Phys. Rep. **336**, 1 (2000).

[5] L. S. Levitov and G. B. Lesovik, Pis'ma Zh. Eksp. Teor. Fiz. **58**, 225 (1993) [JETP Lett. **58**, 230 (1993)]. For a recent review, see L. S. Levitov, in *Quantum Noise in Mesoscopic Systems*, edited by Yu. V. Nazarov (Kluwer, Dordrecht, 2003).

[6] K. Richter and M. Sieber, Phys. Rev. Lett. **89**, 206801 (2002).

[7] P. Braun, S. Heusler, S. Müller, and F. Haake, J. Phys. A: Math. Gen. **39**, L159 (2006).

[8] B. Béri and J. Cserti, Phys. Rev. B **75**, 041308(R) (2007).

[9] J. N. H. J. Cremers, P. W. Brouwer, and V. I. Fal'ko, Phys. Rev. B **68**, 125329 (2003).

[10] S. Heusler, S. Müller, P. Braun, and F. Haake, Phys. Rev. Lett. **96**, 066804 (2006).

[11] I. L. Aleiner and V. I. Fal'ko, Phys. Rev. Lett. **87**, 256801 (2001); **89**, 079902(E) (2002).

[12] R. S. Whitney, P. Jacquod, and C. Petitjean, Phys. Rev. B **77**, 045315 (2008).

[13] P. W. Brouwer, Phys. Rev. B **76**, 165313 (2007).

[14] J. G. G. S. Ramos, A. L. R. Barbosa, and A. M. S. Macêdo, Phys. Rev. B **78**, 235305 (2008).

[15] A. L. R. Barbosa, J. G. G. S. Ramos, and A. M. S. Macêdo, J. Phys. A: Math. Gen. **43**, 075101 (2010).

[16] Yu. V. Nazarov and D. A. Bagrets, Phys. Rev. Lett. **88**, 196801 (2002).

[17] A. M. S. Macêdo, Phys. Rev. B **66**, 033306 (2002).

[18]For a review, see Yu. V. Nazarov and Ya. M. Blanter, *Quantum Transport: Introduction to Nanoscience* (Cambridge University Press, Cambridge, 2009).
[19]G. C. Duarte-Filho, A. F. Macedo Junior, and A. M. S. Macêdo, Phys. Rev. B **76**, 075342 (2007).
[20]A. M. S. Macêdo, Phys. Rev. B **61**, 4453 (2000).
[21]P. W. Brouwer and C. W. J. Beenakker, J. Math. Phys. **37**, 4904 (1996).
[22]M. L. Polianski and P. W. Brouwer, J. Phys. A: Math. Gen. **36**, 3215 (2003).
[23]M. L. Mehta, *Random Matrices*, 3rd ed. (Elsevier, Amsterdam, 2004).
[24]R. S. Whitney, Phys. Rev. B **75**, 235404 (2007).
[25]P. W. Brouwer and S. Rahav, Phys. Rev. B **74**, 085313 (2006).
[26]G. Berkolaiko, J. M. Harrison, and M. Novaes, J. Phys. A: Math. Gen. **41**, 365102 (2008).
[27]B. Béri and J. Cserti, Phys. Rev. B **74**, 235314 (2006).
[28]G. Campagnano and Yu. V. Nazarov, Phys. Rev. B **74**, 125307 (2006).
[29]K. Saito and T. Nagao, Phys. Rev. B **82**, 125322 (2010).
[30]S. Gustavsson, R. Leturcq, B. Simovic, R. Schleser, T. Ihn, P. Studerus, K. Ensslin, D. C. Driscoll, and A. C. Gossard, Phys. Rev. Lett. **96**, 076605 (2006).
[31]S. Gustavsson, R. Leturcq, T. Ihn, K. Ensslin, M. Reinwald, and W. Wegscheider, Phys. Rev. B **75**, 075314 (2007).
[32]Yu. Bomze, G. Gershon, D. Shovkun, L. S. Levitov, and M. Reznikov, Phys. Rev. Lett. **95**, 176601 (2005).
[33]D. M. Zumbühl, J. B. Miller, C. M. Marcus, K. Campman, and A. C. Gossard, Phys. Rev. Lett. **89**, 276803 (2002).
[34]J. B. Miller, D. M. Zumbühl, C. M. Marcus, Y. B. Lyanda Geller, D. Goldhaber-Gordon, K. Campman, and A. C. Gossard, Phys. Rev. Lett. **90**, 076807 (2003).